Modelling the climatic drivers determining photosynthesis and carbon allocation in evergreen Mediterranean forests using multiproxy long time series

[1,*]Gea-Izquierdo G, [2]Guibal F, [3]Joffre R, [3]Ourcival JM, [4]Simioni G, [1]Guiot J

[1]CEREGE UMR 7330, CNRS/Aix-Marseille Université. Europole de l'Arbois BP 80 13545 Aix-en-Provence cedex 4, France. [2]IMBE, CNRS /Aix-Marseille Université UMR 7263 Europole de l'Arbois BP 8013545 Aix-en-Provence cedex 4, France. [3]Centre d'Ecologie Fonctionnelle et Evolutive CEFE, UMR 5175, CNRS - Université de Montpellier - Université Paul-Valéry Montpellier – EPHE, 1919 Route de Mende, 34293 Montpellier Cedex 5, FRANCE. [4]Ecologie des Forêts Méditerranéennes, INRA UR 629, Domaine Saint Paul, 84914 Avignon Cedex 9, France.

[*]Author for correspondence: gea-izquierdo@cerege.fr

Abstract

Climatic drivers limit several important physiological processes involved in ecosystem carbon dynamics including gross primary productivity (GPP) and carbon allocation in vegetation. Climatic variability limits these two processes differently. We developed an existing mechanistic model to analyse photosynthesis and variability in carbon allocation in two evergreen species at two Mediterranean forests. The model was calibrated using a combination of eddy covariance CO_2 flux data, dendrochronological time series of secondary growth and forest inventory data. The model was modified to be climate explicit in the key processes addressing acclimation of photosynthesis and the pattern of C allocation, particularly to water stress. It succeeded to fit both the high- and the low-frequency response of stand GPP and carbon allocation to stem growth. This would support its capability to address both C-source and C-sink limitations. Simulations suggest a decrease in mean stomatal conductance in response to recent

enhancement in water stress and an increase in mean annual intrinsic water use efficiency (iWUE) in both species during the last 50 years. However, this was not translated into a parallel increase in ecosystem water use efficiency (WUE). Interannual variability of WUE followed closely that of iWUE at both sites. Nevertheless, long-term decadal variability of WUE followed the long-term decrease in annual GPP matching the local trend in annual precipitation observed since the late 1970s at one site. In contrast, at the site where long-term precipitation remained stable, GPP and WUE did not show a negative trend and the trees buffered the climatic variability. In our simulations these temporal changes would be related to acclimation processes to climate at the canopy level including modifications in LAI and stomatal conductance, but also partly related to increasing [CO_2] because the model includes biochemical equations where photosynthesis is directly linked to [CO_2]. Long-term trends in GPP did not match those in growth, in agreement with the C-sink hypothesis. There is a great potential to use the model with abundant dendrochronological data and analyse forest performance under climate change. This would help to understand how different interfering environmental factors produce instability in the pattern of carbon allocation, hence the climatic signal expressed in tree-rings.

Keywords: *Pinus halepensis*, *Quercus ilex*, process-based model, dendrochronology, eddy covariance; global change.

Introduction

Global change challenges forest performance because it can enhance forest vulnerability (IPCC 2013). Trees modify multiple mechanisms at different scales to tackle with environmental stress, including changes in photosynthesis and carbon allocation within plants (Breda et al. 2006; Niinemets 2007; Chen et al. 2013). Many factors affect the different physiological processes driving forest performance. Among them, the net effect of rising CO_2 mixing ratio ($[CO_2]$) and climate change is meaningful to determine the forests' capacity of acclimation to enhanced xericity (Peñuelas et al. 2011; Keenan et al. 2011; Fatichi et al. 2014). Forest process-based models have been developed to mimic these mechanisms. They can include different levels of complexity but generally implement calculations of leaf photosynthesis up-scaled to the canopy and carbon allocated to different plant compartments (Le Roux et al. 2001; Schaefer et al. 2012; De Kauwe et al. 2013). Although there is evidence that the tree performance depends to some extent on stored carbohydrates (Breda et al. 2006; McDowell et al. 2013; Dickman et al. 2014), these models have received some criticism when used to understand plant performance in response to climate change. This is in part because they are C-source oriented, therefore can exhibit certain limitations to represent the C-sink hypothesis (i.e. that growth rates are limited by environmental factors such as water stress, minimum temperature or nutrient availability rather than by carbohydrate availability) and address dysfunctions related to the tree hydraulics (Millard et al. 2007; Breshears et al. 2009; Sala et al 2012; Körner et al. 2013; McDowell et al. 2013; Fatichi et al. 2014).

Complex process-based models profit from multiproxy calibration, particularly when such data are applied at different spatio-temporal scales (Peng et al. 2011). The temporal scale can be approached using time growth series of dendrochronological data.

71 However the analysis of the past always adds uncertainties related to the influence of
72 unknown stand conditions to properly scale productivity. Flux data including stand
73 productivity can be estimated using the eddy covariance technique (Baldocchi 2003).
74 These data overcome many of the limitations of dendroecological data (e.g. intra-annual
75 resolution, control of stand conditions and scaling of net productivity) but they lack
76 their spatial and temporal coverage. Thus, CO_2 flux data can be used to implement
77 unbiased models of canopy photosynthesis, and then combined with dendroecological
78 data to study how carbon is allocated to stem growth as a function of environmental
79 forcing (Friedlingstein et al. 1999; Chen et al. 2013, McMurtrie & Dewar 2013).
80 Mechanistic models can be also used to analyse the environmental factors
81 determining instability in the climate-growth response (D'Arrigo et al. 2008). Different
82 process-based models have been applied with dendroecological data used either in
83 forward or inverse mode (see Guiot et al. 2014 for a review). Among these models, the
84 process-based model MAIDEN (Misson 2004) was originally developed using
85 dendroecological data. The model explicitly includes [CO_2] to calculate photosynthesis
86 (hence its influence on carbon allocation) and includes a carbohydrate storage reservoir.
87 The latter being one of its strengths compared to other models (Vaganov et al. 2006;
88 Sala et al. 2012; Guiot et al. 2014). It has been previously employed to analyse growth
89 variability in one temperate and two Mediterranean species (Misson et al. 2004;
90 Gaucherel et al. 2008) and recently on inverse mode (also including C and O stable
91 isotopes) to reconstruct past climate (Boucher et al. 2014). However, it requires further
92 development to ensure that it provides unbiased estimates of forest productivity and
93 assesses uncertainties in the response of trees to climatic variability at a greater spatial
94 scale at the regional level. Particularly, its parameterization would need improvement if

95 the model is applied to assess how climate modulates forest performance and the pattern
96 of C allocation within plants (Niinemets & Valladares 2004; Fatichi et al. 2014).
97 In this study we use multiproxy data to develop a process-based model and
98 investigate how evergreen Mediterranean forests have modified stand photosynthesis
99 and carbon allocation in response to interacting climatic factors and enhanced [CO_2] in
100 the recent past. The first objective was to develop a process-based model based on
101 MAIDEN (Misson 2004). Within the new version of the model, photosynthesis, carbon
102 allocation, canopy turnover and phenology are now calculated using climate explicit
103 functions with a mechanistic basis. The model is adapted to give unbiased estimates of
104 canopy photosynthesis and stem growth using instrumental data. Specifically, within the
105 new model formulation: (1) photosynthesis is penalized by prolonged water stress
106 conditions through reductions in leaf area index (LAI) and maximum photosynthetic
107 capacity; (2) the pattern of carbon allocation is directly determined by soil water content
108 (i.e. water stress) and temperature through nonlinear relationships; (3) these
109 relationships can be contrasting for different phenophases and affect independently
110 photosynthesis and the pattern of C allocation. Once the model was developed, a second
111 objective was to analyse how [CO_2] and climatic variability affect the temporal
112 instability in annual forest productivity, water use efficiency and carbon allocation. We
113 hypothesise that they will exhibit differences in their long-term variability in relation to
114 recent climate change driven by different functional acclimation processes within trees.
115
116 **Material and methods**
117 *Study sites and climatic data*
118 The study sites were two evergreen Mediterranean monitored forests in Southern
119 France where CO_2, water vapour and energy fluxes are measured using the Eddy

120 covariance technique (Baldocchi 2003). Both sites are included in FLUXNET
121 (http://fluxnet.ornl.gov/). The first site Fontblanche (43.2º N, 5.7º E, 420 m) is a mixed
122 stand where *Pinus halepensis* Mill. dominates the open top canopy layer reaching about
123 12 m, *Quercus ilex* L. forms a lower canopy layer reaching about 6 m and there is a
124 sparse shrub understory including *Quercus coccifera* L. (Simioni et al. 2013). The
125 second site, Puechabon (43.4ºN, 3.4º E, 270 m), is a dense coppice in which overstory is
126 dominated by *Q. ilex* with density around 6,000 stems/ha (Rambal et al. 2004; Limousin
127 et al. 2012). Both forests grow on rocky and shallow soils with low retention capacity
128 and of Jurassic limestone origin. The climate is Mediterranean, with a water stress
129 period in summer, cold or mild winters and most precipitation occurring between
130 September and May. Meteorological data were obtained from the neighbouring stations
131 of St. Martin de Londres (for Puechabon) and Aubagne (for Fontblanche). According to
132 those data Puechabon is colder and receives more precipitation than Fontblanche (Table
133 1). Meteorological data showed a decrease in total rainfall since the 1970s in Puechabon
134 but no trend in Fontblanche. Both sites exhibit a positive trend in temperatures more
135 evident for the maximum values (Figure A1).

136 We assumed that GPP is driven by the top pine and/or oak layers and that the
137 percentage of LAI related to the understory shrub layer will behave like that of the oak
138 species (evergreen, shrubby). For Fontblanche we considered a maximum leaf area
139 index (LAI_{max}) of 2.2 $m^2 \cdot m^{-2}$ (3 $m^2 \cdot m^{-2}$ plant area index, PAI), composed by a 70% of
140 pine and 30% of oak (Simioni et al. 2013). For Puechabon we considered a LAI_{max} of
141 2.0 $m^2 \cdot m^{-2}$ (2.8 $m^2 \cdot m^{-2}$ PAI) monospecific of *Q. ilex* (Baldocchi et al. 2010; Limousin et
142 al. 2012). Specific leaf area (*SLA*) considered was 0.0045 $m^2 \cdot g^{-1}$ for *Q. ilex* and 0.0037
143 $m^2 \cdot g^{-1}$ for *P. halepensis,* respectively (Hoff & Rambal 2003; Maseyk et al. 2008).
144

145 *The model*

146 We used MAIDEN (Misson 2004), a stand productivity mechanistic model driven
147 by a number of functions and parameters representing different processes. The model
148 inputs are precipitation, maximum and minimum temperature and [CO_2] with a daily
149 time step. This model has been previously implemented for monospecific forests
150 including two oaks and one pine species using dendroecological chronologies of growth
151 and, when available, stand transpiration estimates from sap-flow sensors (Misson et al.
152 2004; Gaucherel et al. 2008). However, the model has never been compared to actual
153 CO_2 flux data to ensure that it provides unbiased estimates of forest productivity. In this
154 study, the model was further developed to match ground-based observations and
155 generalize model use by modifying the photosynthesis and allocation modules
156 (including the different phenophases) in relation to climatic drivers. To properly scale
157 model outputs and get unbiased estimates of stand productivity we used CO_2 eddy
158 covariance fluxes (Baldocchi 2003). Different parameters were calibrated to different
159 data sources, including some species-dependent and some site-dependent parameters, as
160 follows. The transpiration rate (E) of day *i* is calculated using a conductance approach
161 as $E(i)=g_s(i)\cdot VPD(i)/P_{atm}(i)$, where P_{atm} is atmospheric pressure and g_s and *VPD* are
162 stomatal conductance and vapour pressure deficit, respectively, as described below
163 (Misson 2004). Those other equations used to calculate micrometeorological covariates,
164 soil humidity and photosynthetic active radiation, as well as those functions describing
165 the water cycle (including soil evaporation and plant transpiration) are explained in the
166 original model formulation from Misson (2004). Therefore they won't be described
167 here. The rest of the model was modified as follows.

168

169 *Modelling the effect of climatic forcing on photosynthesis*

Leaf photosynthesis (A_n) is calculated based on the biochemical model of Farquhar et al. (1980). A_n is a function of the carboxylation (V_c), oxygenation (V_o) and leaf dark respiration rates (R_d): $A_n=V_c-0.5V_o-R_d$; where photosynthesis at day i is limited by either the rate of carboxylation when Rubisco is saturated (W_c) or when it is limited by electron transport (W_j), i.e. $A_c=V_c-0.5V_o=min\{W_c, W_j\}$. R_d was considered a fixed function of A_c ($0.006 \cdot A_c$), because it performed better in our daily model than exponential formulations as a function of temperature (Sala & Tenhunen 1996; De Pury & Farquhar 1997; Bernacchi et al. 2001). Following De Pury & Farquhar (1997):

$$W_c(i) = \frac{V_{cmax}(i) \cdot (C_i(i) - \Gamma(i))}{C_i(i) + K_c(i)\left(1 + \frac{[O_2]}{K_o(i)}\right)} \qquad [E1],$$

$$W_j(i) = \frac{J_{max}(i) \cdot (C_i(i) - \Gamma(i))}{4C_i(i) + 8\Gamma(i)} \qquad [E2];$$

where C_i is the CO_2 intercellular concentration, Γ is the $[CO_2]$ compensation point for photosynthesis in the absence of dark respiration, and K_c and K_o are the kinetic Michaelis-Menten constants for carboxylation and oxygenation, respectively. V_{cmax} and J_{max} are temperature dependent parameters as follows. Photosynthesis is known to respond to the carbon concentration within chloroplasts C_c rather than to C_i. We keep through the paper the notation presented here in [E1] and [E2] but discuss below how mesophyll conductance is taken into account empirically in relation to water stress when calculating g_s and acknowledge the possible limitations of our approach (Reichstein et al. 2002; Grassi & Magnani 2005; Flexas et al. 2006; Sun et al. 2014).

Climate influences leaf photosynthesis calculations through the temperature dependence of different parameters (Bernacchi et al. 2001; Nobel 2009). Γ, K_c and K_o were modelled using Arrhenius functions of daily mean temperature (T_{day}, in ºC) with parameters as in De Pury & Farquhar (1997). We modelled J_{max} as a fixed rate of V_{cmax} ($J_{max(i)}=J_{coef} \cdot V_{cmax(i)}$) after comparing with different temperature dependent

192 formulations (De Pury & Farquhar 1997; Maseyk et al. 2008). The model behaviour
193 was better when the temperature dependence of V_{cmax} was modelled using a logistic
194 function (Gea-Izquierdo et al. 2010) rather than an exponential function as in Misson
195 (2004):

$$V_{cmax}(i) = \frac{V_{max}}{\left(1 + \exp\left(V_b \cdot \left(\left(T_{day}(i) + 273\right) - V_{ip}\right)\right)\right)} \cdot \theta_p \quad \text{[E3]};$$

196 V_{max}, V_b and V_{ip} are parameters to be estimated, with V_{max} being the asymptote and V_{ip}
197 the inflection point. θ_p is a soil water stress function dependent on soil moisture
198 conditions of the previous year. It takes into account down-regulation of photosynthesis
199 in response to protracted drought through its impact on the photosynthetic capacity of
200 active LAI in evergreen species caused by constraints in V_{cmax} produced by irreversible
201 photoinhibition, modifications in leaf stoichiometry and/or aging of standing foliage
202 through lower leaf replacement rates in response to long-term water stress (Sala &
203 Tenhunen 1996; Niinemets & Valladares 2004; Niinemets 2007; Vaz et al. 2010).
204 $\theta_p = 1 - exp(p_{str} \cdot SWC_{180})$ [E4], where p_{str} is a parameter to be estimated and
205 SWC_{180} is the mean soil water content (mm) from July to December of the previous
206 year.

207 Photosynthesis is coupled to stomatal conductance calculation, which is estimated
208 using a modified version of the Leuning (1995) equation:

$$g_s(i) = \frac{g_1 \cdot A_n(i)}{(C_s(i) - \Gamma(i)) \cdot (1 + VPD(i)/VPD_0)} \cdot \theta_g(i) \qquad \text{[E5]},$$

209 g_1 and VPD_0 are parameters, VPD(i) is daily vapour pressure deficit, C_s is the leaf
210 surface [CO_2]; θ_g is a non-linear soil water stress function as:

$$\theta_g(i) = \frac{1}{1 + \exp(soil_b \cdot (SWC(i) - soil_{ip}))} \qquad \text{[E6]},$$

211 $soil_b$ and $soil_{ip}$ are parameters and *SWC(i)* is daily soil water content (mm). θ_g accounts
212 for variability in gas exchange under drought conditions which cannot be taken into
213 account only through stomatal control, e.g. related to mesophyll conductance or
214 stomatal patchiness. Therefore, with this empirical expression we partly represent the
215 effect of CO_2 fractionation during mesophyll conductance under water stress,
216 acknowledging that this will be likely more complex under environmental stress
217 (Reichstein et al. 2002; Grassi & Magnani 2005; Flexas et al. 2006; Sun et al. 2014).
218 The coupled photosynthesis-stomatal conductance system of equations was estimated
219 separately for sun and shade leaves. Canopy photosynthesis was integrated using LAI
220 divided into its sunlit and shaded fractions (De Pury & Farquhar 1997). Transmission
221 and absorption of irradiance was calculated following the Beer-Lambert law as a
222 function of LAI, with $LAI_{sun}=(1-\exp(-LAI))\cdot K_b$ (K_b is the beam light extinction
223 coefficient, which was set to 0.8) and $LAI_{shade}=LAI-LAI_{sun}$ (Misson 2004). In the mixed
224 stand (Fontblanche), photosynthesis was calculated separately for *Q. ilex* and *P.*
225 *halepensis*, and then integrated to get stand estimates of forest productivity.
226
227 *Modelling the effect of climatic forcing on carbon allocation*
228 The model allocates daily carbon assimilated either to the canopy, stem, roots or
229 storage of non-structural carbohydrates (NSC) to mimic intra-annual carbohydrate
230 dynamics (Misson 2004; Dickman et al. 2014). Although trees can store carbon within
231 different above-ground and below-ground compartments (Millard et al. 2007), carbon
232 storage is treated as a single pool within the model. Tree autotrophic respiration (R_a, in
233 addition to R_d) is modelled as a function *f(i)* of daily photosynthesis and maximum daily
234 temperature (T_{max}) (Sala & Tenhunen 1996; Nobel 2009) as:
235 $R_a(i) = A_n(i) \cdot \max\{0.3, f(i)\}$, with $f(i) = 0.47 \cdot (1 - \exp\left(p_{respi} \cdot T_{max}(i)\right)$ [E7];

where p_{respi} is a parameter. Net photosynthesis is calculated for day i as $A_N(i)=A_n(i)-R_a(i)$. This assumption means that respiration would be considered nil when there is no photosynthesis, hence maintenance respiration would not be taken into account those days. Although this could bias the overall carbon balance, we assume that this effect will be very reduced in the studied forests because they present photosynthetic activity all year round (see results). The model simulates several phenological phases during the year (see Figure 1):

[P1] winter period where all photosynthates assimilated daily, $A_N(i)$, are allocated to the storage reservoir (NSCs) but there is no accumulation of growing degree days (GDD).

[P2] winter period where all $A_N(i)$ are allocated to storage (i.e. the same as in [P1]) but in opposition to [P1] there is active accumulation of GDD which define the threshold GDD_1 to trigger the next phenophase [P3] (budburst, leaf-flush).

[P3] budburst, where carbon available $C_T(i)=A_N(i)+C_{bud}$ (C_{bud} is daily C storage utilized from buds, a parameter) is either allocated to the canopy, to roots or to the stem.

[P4] once the canopy has been completed in [P3], the next phenophase [P4] starts; in this period, daily photosynthates $A_N(i)$ are allocated either to the stem or to storage;

[P5] the last phenophase [P5] starts when the photoperiod (parameter) crosses a minimum threshold in fall. In this phase root mortality occurs. Otherwise [P5] is similar to [P1] and [P2], in the sense that all $A_N(i)$ is used for storage until next year [P3] starts.

Allocation of carbon to different plant compartments is complex because it can be decoupled from photosynthetic production depending on different factors, some of them climatic, acting at different temporal scales (Friedlingstein et al. 1999; Sala et al. 2012; Chen et al. 2013; McMurtrie & Dewar 2013). In this new version of the model we set the different allocation relationships as nonlinear functions of temperature and soil water content, $h(i)=f_1(T_{max})\cdot f_2(SWC)$, in [P3] and [P4] following the functional

relationships described in Gea-Izquierdo et al. (2013). This means that now we take into account homeostatic acclimation processes at the canopy level related to LAI dependence on water availability (Hoff & Rambal 1993; Sala & Tenhunen 1996; Reichstein et al. 2003). LAI is negatively related to long-term drought because litterfall is negatively linked to water stress (Limousin et al. 2009; Misson et al. 2011) and bud size depends on climate influencing the period of bud formation (Montserrat-Marti et al 2009). Therefore the actual carbon that can be allocated to the canopy in [P3] of year *j* ($AlloC_{canopy}(j)$) was set as a function of previous year moisture conditions ($\theta_{LAI}(j)$), and maximum carbon that can be allocated to the canopy ($MaxC_{canopy}$). $MaxC_{canopy}$ is calculated from LAI_{max} and *SLA*, and $AlloC_{canopy}(j) = \theta_{LAI}(j) \cdot MaxC_{canopy}$, where:

$$\theta_{LAI}(j) = \left(1 - 2 \cdot \frac{p_{LAI} - SWC_{250}}{p_{LAI}}\right), \text{constrained to } \theta_{LAI}(j) \in [0.7, 1.0] \quad \text{[E8]}$$

p_{LAI} is a parameter to be calibrated representing the threshold over which $\theta_{LAI}(j) = 1$ and SWC_{250} is mean soil water content for May-December of previous year.

Leaf turnover is variable within years and partly related to water availability (Limousin et al. 2009, 2012). We considered a mean leaf turnover rate of 3 years for pines and 2 for oaks. To model within year variability in leaf phenology (i.e. leaf growth and litterfall) we followed Maseyk et al. (2008) and Limousin et al. (2009) (Figure 1). C allocation to the canopy (i.e. including primary growth) in [P3] is calculated as: $C_{canopy}(i) = C_T(i) \cdot (1 - 0.2 \cdot h_{3\_1}(i)) \cdot Ratio_{root/leaf}^{-1}$; $Ratio_{root/leaf}$ was fixed to 1.5 for both species (Misson et al. 2004; Ourcival, unpublished data), and:

$$h_{3\_1}(i) = (1 - \exp(p_{3moist} \cdot SWC(i)) \cdot \left(\exp\left(-0.5 \cdot \left(\frac{T_{max}(i) - p_{3temp}}{p_{3sd}}\right)^2\right)\right) \quad \text{[E9]},$$

p_{3moist}, p_{3temp} and p_{3sd} are parameters representing the scale of the *SWC* and the optimum and dispersion of the T_{max} functions respectively. The carbon allocated to the stem (C_{stem}) in [P3] is $C_{stem}(i) = C_T(i) \cdot 0.2 \cdot h_{3\_1}(i) \cdot h_{3\_2}(i)$, where:

$$h_{3\_2}(\mathrm{i}) = (1 - \exp(st_{3moist} \cdot SWC(i)) \cdot \left(\exp\left(-0.5 \cdot \left(\frac{T_{max}(i) - st_{3temp}}{st_{3sd\_temp}}\right)^2\right)\right) \quad \text{[E10]};$$

with h_{3_1}(i) as in [E9]; st_{3moist}, st_{3temp} and st_{3sd_temp} are parameters as in h_{3_1}(i). The carbon allocated to roots in [P3] is set complementary to that of the other compartments to close the carbon budget within the tree, i.e.: C_{roots}(i)=C_T(i)-C_{stem}(i)-C_{canopy}(i).

Finally, in [P4] carbon assimilated daily A_N(i) is allocated either to stem growth or to storage until changing to [P5]. There since in [P1] and [P2] again all A_N(i) is only allocated to storage until [P3] next year (Misson 2004). In [P4], the amount of carbon to be allocated to stem growth is now also set as a function of climatic forcing:

C_{stem}(i)= A_N(i)·(1-h_4(i)) and C_{stor}(i)= A_N(i)·h_4(i), with:

$$h_4(\mathrm{i}) = \left(1 - \exp(st_{4temp} \cdot T_{max}(i)\right) \cdot \left(\exp\left(-0.5 \cdot \left(\frac{SWC(i)}{st_{4sd\_moist}}\right)^2\right)\right) \quad \text{[E11]};$$

st_{4temp} and st_{4sd_temp} are parameters as from [E10].

Eddy covariance CO_2 flux and dendrochronological data

The process-based model was calibrated using daily gross primary productivity (GPP), dendrochronological data and inventory data. To develop the model, in a first step those functions used to model daily stand photosynthesis (i.e. [E1] to [E9]) were calibrated against GPP values. GPP estimates were obtained from half-hourly net CO_2 flux measurements (NEP). GPP was obtained as the difference between measured net ecosystem productivity and calculated ecosystem respiration (Reichstein et al. 2005). Negative GPP values were corrected following Schaefer et al. (2012). Half-hourly GPP data were integrated to obtain daily estimates for the period 2001-2013 (Puechabon, methods detailed in Allard et al. (2008)) and 2008-2012 (Fontblanche) (Table 1).

In a second step, those functions used to model how carbon assimilated and/or storage is allocated to growth of the tree stem (i.e. [E10] and [E11]) were developed

using calculated annual stem biomass increment time series. Stem biomass increment chronologies were built combining dendroecological data and forest inventory data collected at each site. We built one chronology for *Q. ilex* in Puechabon, a second for *Q. ilex* in Fontblanche and a third one for *P. halepensis* at Fontblanche (Figure 2). For pines, two perpendicular cores were extracted using an increment borer from 25 trees in fall 2013 whereas for oaks we used crossections. In Fontblanche, 15 oak stems were felled and basal sections collected in spring 2014. A total of 17 oak stems from Puechabon were logged in 2005 and 2008. The age and diameter distributions of the studied forests are depicted in Figure A2.

All samples were processed using standard dendrochronological methods (Fritts 1976). Annual growth (RW) was measured using a stereomicroscope and a moving table switched to a computer. RW crossdating was visually and statistically verified. RW estimates were transformed to basal area increments (BAI, $cm^2 \cdot year^{-1}$). Mean BAI chronologies were obtained by averaging individual tree BAI time series. In Fontblanche BAI during the period 1987-1995 was standardized relative to the mean calculated after excluding that period (Figure 2). BAI data were standardized because we did not find a climatic explanation for the abrupt growth peak observed in Fontblanche during that period (Figure 2). Therefore we assumed that it had been caused by a release event (i.e. reduction in competition) produced by the death of neighbours as a consequence of winter frost during 1985 and 1987 (Vennetier, pers. comm., 2014). These two frosts were reflected by the presence of characteristic frost rings in most individuals from Fontblanche.

To scale BAI chronologies to the same units as annual stem biomass (which is an output of the model) we used plot inventory data collected around the flux towers at the two sites. Inventory data included stem diameter for all trees and tree height collected

for a subsample every two years during 2007-2011 in Fontblanche, and annual diameter estimates for the period 1986-2011 for Puechabon. Individual annual biomass increments were estimated by subtracting stem biomass at consecutive years and then stand stem biomass increment (SBI, g C m^{-2}·$year^{-1}$) built integrating plot data. Stem biomass was calculated using allometric functions. For pines, we calculated stem biomass using diameter and estimated stem height assuming that the tree bole follows a paraboloid shape (Li et al. 2014). For oaks, stem biomass was calculated following Rambal et al. (2004). Once SBI had been estimated for the years when we had available inventory data, BAI chronologies were correlatively scaled to SBI units (g C m^{-2}·$year^{-1}$). We built two mean stand SBI chronologies, one for each site, meaning that we analysed carbon allocation within stands, not differentiating between species in Fontblanche. These two SBI chronologies were used to calibrate sitewise [E10] and [E11].

Model development and analyses

Parameters were selected according to the ecological characteristics of the species, exploring the model using comprehensive sensitivity analysis to sequentially optimize groups of parameters. In a first step, a group of common parameters (those included in [E2] to [E8]) was selected using GPP data from Fontblanche (Table 2). The species-dependent parameters selected for *Q. ilex* in this first step were independently validated when applied in Puechabon (those in Table 2 common for the two sites). In a second step, a subset of site-dependent parameters was calibrated against GPP and SBI data. Four from [E6] and [E9] were calibrated using GPP data, and five parameters in [E10] and [E11] were calibrated using stem biomass increment data (Table 2). The local

parameters were calibrated constrained to an ecologically realistic range using a global optimization algorithm and maximum likelihood principles (Gaucherel et al. 2008).

To compare model output with stem biomass chronologies as estimated from dendroecological data we used only the period where we had available daily meteorological data (1960-2013), which was also a period that did not include juvenile years with increasing BAI (BAIs reached an asymptote after increasing the first 15-20 juvenile years, Figure 2). The model does not take into account how size differences in allometry or ontogeny affect carbon allocation (Chen et al. 2013). We tried to keep the model as simple as possible also because we had no such data to calibrate ontogenic effects. Hence the model is designed for non-juvenile stands with canopies that reached a steady state with asymptotic LAI_{max}. For the same reasons it does not take into account how changes in management affect carbon allocation. The model was analysed in terms of goodness of fit. Additionally, for the period where we had available daily meteorological data we simulated time series of GPP, ecosystem water use efficiency ($WUE = GPP/ET$, with ET=actual evapotranspiration) and intrinsic water use efficiency of sun leaves ($iWUE = A_N/g_s$) calculated following Beer et al. (2009).

Results

The studied evergreen forests exhibit a bimodal pattern in GPP with maxima in spring and autumn (Figure 3) as often observed in Mediterranean ecosystems (e.g. Baldocchi et al. 2010). GPP was above zero almost every day of the year, including winter, particularly in the milder site, Fontblanche (Table 1). This means that there is active photosynthesis all year round in these evergreen forests, including both periods of climatic stress with low temperature and short photoperiod in winter, and with low moisture availability in summer (Figure 3). Mean annual GPP was 1431.4±305.4 g C m^{-}

^{2} year^{-1} and precipitation 642.7±169.7 mm in Fontblanche; whereas it was 1207.3±206.7 g C m^{-2} year^{-1} and 1002.6±328.2 mm in Puechabon (see Table 1 for more details). Mean GPP was higher at Fontblanche because carbon assimilation was greater in the low temperature winter period but similar the rest of the year (Figure 3). Stem growth did not show any long-term (decadal) growth trend for any of the species studied (Figure 2).

The model accurately represented the low frequency response of GPP: both the seasonal variability in GPP within years and variability in GPP among years (Figure 4). The model explained over 50% of the annual biomass growth variance, and 46% and 59% of daily GPP in Fontblanche and Puechabon, respectively (Figure 4). This means that we were able to mimic the daily, seasonal and long-term trends in stand productivity with unbiased estimates but also to model how carbon is allocated to stem growth along the year at the different phenophases described. The model assumed species-specific carbon allocation responses set to the different plant compartments as nonlinear functions of temperature and soil moisture. These relationships were biologically meaningful in the sense that photosynthesis and carbon allocation could be decoupled to some extent as a function of climatic variability. Once the canopy has been formed in spring, the model allocated more carbon to the stem and less to storage when less severe climatic stress occurs, i.e. with decreasing temperatures and more humid conditions (Figure 5).

Both sites exhibited an increase in temperature particularly evident in the maximum values but only Puechabon suffered a decrease in annual precipitation between 1960 and 2012 (Figure A1). In the model, the studied forests acclimated to changing climatic conditions in the last decades coupling different physiological traits and simulated annual GPP greatly followed the overall trends in precipitation observed. In Fontblanche, which is milder and receives less precipitation, GPP remained stable since

the 1960s and presented no apparent long-term trend (Figure 6). In contrast, in the coldest and rainiest site (Puechabon) the model simulated a decrease in GPP (Figure 6), which was driven by the prevailing decrease in precipitation observed since the 1970s (Figure A1; Figure 6). This reduction of GPP was partly a consequence of decreased LAI in response to enhanced long-term water stress (Figure A3; Limousin et al. 2009; Misson et al. 2011). Simulated long-term decadal trends in mean annual stomatal conductance were similar and decreasing at the two sites with greater water stress as a consequence of enhanced temperatures (Figure 6). The two species studied showed a long-term increase in simulated iWUE (Figure 7) following the decrease in simulated g_s (Figure 6). The interannual variability of WUE and iWUE were highly and positively correlated (Figure 7). However, in the long-term they followed a different pattern particularly in Puechabon where there was a recent decline in WUE (not observed in iWUE) forced by trends in ET and GPP (Figure 7). This means that the recent reduction in simulated GPP was proportionally greater than that of simulated ET (Figure 6; Figure A3).

Discussion

Linking photosynthetic production to carbon allocation as a function of climate

The model calculates stand productivity and carbon allocation to stem growth in response to climate and [CO_2] with realism. It is particularly well suited to mimic the effect of water stress in plant performance by the explicit assessment of different acclimation processes at the canopy level including changes in stomatal conductance and photosynthetic capacity (Sala & Tenhunen 1996; Reichstein et al. 2003; Limousin et al. 2010; Misson et al. 2011). Additionally, the model simulates carbohydrate storage dynamically as a function of environmental variability. Climate can affect differently

the carbon dynamics and pattern of C-allocation to different tree compartments at different phenophases. In the model the storage reservoir is an active sink for assimilated carbon during some periods of the year and a source in spring to be used in primary and secondary growth (Figure A5). Additionally stem growth is limited by climatic constraints (in [P3] and [P4]) rather than just by the amount of available carbohydrates (Millard et al. 2007). This means that water stress and optimum temperature directly affect the modelled processes assuming that cell-wall expansion in the xylem can relate to climatic variability differently than photosynthetic production (Sala et al. 2012). The model showed C-limitation (for primary growth) the years when LAI_{max} was not achieved (i.e. a limitation in LAI is driven by limitations in the C supply in spring), e.g. all years in Puechabon for the period shown in Figure A5 (1995-2012) but only those years in Fontblanche when the minimum value considered as a threshold was reached. Therefore both C-source (photosynthesis) and C-sink (just related to growth, other sinks such as volatile organic compounds or root exudates are not explicitly included in the model) limitations can be assessed at different years within one site and even at different periods within the same year (Millard et al. 2007; Sala et al. 2012; Chen et al. 2013; Fatichi et al. 2014). This hypothesis seems plausible as drought stress affects both C-source (e.g. through reduced stomatal conductance) and C-sink limitations (e.g. cell water turgor, hydraulic performance) (McDowell et al. 2013). Whether the pattern of C-storage simulated is realistic is something that needs to be validated against actual data. However, the flexible way in which stored C is modelled has much potentiality to improve ecosystem models that only view a carbon-source limitation (Sala et al. 2012; Friend et al. 2014).

Water stress is generally considered the greatest limitation for Mediterranean ecosystems, driving an intimate relation between precipitation and both growth and

457 photosynthesis (Breda et al. 2006; Pereira et al. 2007; Baldocchi et al. 2010; Gea-
458 Izquierdo & Cañellas 2014). Our results show that a long-term decrease in precipitation
459 triggered a decrease in simulated GPP at the more rainy and coldest site. However, this
460 decline was not expressed in the growth-trends. This means that long-term productivity
461 and allocation of C to secondary growth were decoupled and did not match (Sala et al.
462 2012; Chen et al. 2013; Fatichi et al. 2014). The existence of trade-offs between carbon
463 assimilation and allocation in relation to environmental variability suggests caution
464 when using growth as a direct proxy to investigate stand productivity dynamics (e.g.
465 Piovesan et al. 2008; Peñuelas et al. 2008; Gea-Izquierdo & Cañellas 2014). GPP was
466 greater in the site receiving less precipitation, which could be related to differences in
467 soil retention capacity. However both soils are calcareous, shallow and stony and
468 differences in GPP were greatly explained by less limitation for carbon assimilation of
469 low winter temperatures at the warmest site (Fontblanche). They can also be a result of
470 different species composition (oak vs. pine-oak). LAI is greater at the site yielding
471 higher annual GPP. Nonetheless, had this factor been responsible for the observed
472 differences in winter photosynthesis, there would have also been differences in spring
473 photosynthesis, which was not the case (Figure 3).

474 A better understanding of the underlying processes determining carbon allocation
475 will benefice process-based models (Sala et al. 2012; Fatichi et al. 2014). Model
476 parameters were within the range found in the literature, bearing in mind that using a
477 daily time step to study differential processes or not distinguishing between leaf ages
478 will affect the scaling of parameters such as J_{max}, V_{cmax} or R_d (De Pury & Farquhar 1997;
479 Grassi & Magnani 2005; Masseyk et al. 2008; Vaz et al. 2010). Daily climatic data are
480 readily available at a greater spatial scale than data with a higher temporal resolution,
481 which increases applicability of daily models. Model performance could be improved

482 by addressing respiration changes related to ontogeny and allometry, nutrient limitations
483 (e.g. N/P) on photosynthesis, or including more complex up-scaling of leaf-level
484 photosynthesis (Niinemets et al. 1999; Niinemets 2007; Chen et al. 2013; McMurtrie &
485 Dewar 2013). However, it is difficult to find suitable data to calibrate such processes.
486 Similarly, it would be challenging to include allocation to reproductive effort in the
487 carbon budget. This is because, even if it is influenced by water stress in the studied
488 forests (Pérez-Ramos et al. 2010), there is still great uncertainty in the causal factors
489 driving multi-annual variability in fruit production (Koenig and Knops 2000).
490 Addressing stand dynamics would also help to generalize model applicability. Stand
491 disturbances modifying stand competition can leave an imprint in growth for more than
492 a decade whereas they do not seem to affect stand GPP over more than one or two years
493 if the disturbance is moderate (Misson et al. 2005; Granier et al. 2008). In response to
494 changes in competition the trees modify the carbon allocation pattern or keep the
495 root:shoot ratio constant to enhance productivity on a per-tree basis but up to an
496 asymptotic stand GPP. Still, the model behaviour was good compared with other studies
497 that addressed ontogenic changes in the carbon-allocation response to photosynthesis
498 (Li et al. 2014) and similar or better than that of other mechanistic approaches calibrated
499 to standardized dendroecological data (Misson et al. 2004; Evans et al. 2006; Gaucherel
500 et al. 2008; Tolwinski-Ward et al. 2011; Touchan et al. 2012).
501
502 *Forest performance in response to recent climate change and [CO_2] enhancement*
503 Few studies under natural conditions observed a net increase of growth rates in
504 response to enhanced [CO_2] levels since the late 1800s, meaning that other factors such
505 as water stress and/or N/P were more limiting for photosynthesis and/or allocation to
506 growth than [CO_2] (Niinemets et al. 1999; Peñuelas et al. 2011; McMurtrie & Dewar

507 2013; Lévesque et al. 2014). Yet the forests have increased their iWUE. This can be
508 partly a passive consequence of enhanced [CO_2] but higher iWUE observed in more
509 water stressed sites suggests that climate is co-responsible for an active acclimation of
510 physiological plant processes (Keenan et al. 2013; Leonardi et al. 2013; Saurer et al.
511 2014). These processes would include a higher stomatal control like in our results where
512 in turn we did not observe any increase in long-term carbon assimilation. The mean
513 annual stomatal conductance simulated was driven by climate but also decreased
514 simultaneously in time with increasing [CO_2] (Appendix A4). Furthermore, there is
515 debate on whether there has been an increase in ecosystem WUE in response to recent
516 changes in [CO_2] under a warming climate (Beer et al. 2009; Reichstein et al. 2002;
517 Keenan et al. 2013). In our results the high-frequency of WUE followed that of iWUE,
518 but there was some mismatch between the two traits in the low-frequency. We observed
519 no dominant time trends in simulated annual WUE for the period 1980-2000 at the site
520 where precipitation remained stable, whereas there was a decrease in WUE following
521 that in GPP particularly evident in the site experiencing a drier climate in recent years.
522 This trend was not observed in iWUE, which means that reductions in GPP and g_s were
523 proportionally greater than those in ET (Figure 6, Figure 7, Appendix A3).

524 Higher [CO_2] concentrations enhance photosynthesis with the equations used to
525 calculate leaf photosynthesis in biochemical models (e.g. Gaucherel et al. 2008; Keenan
526 et al. 2011; Leonardi et al. 2013; Boucher et al. 2014). Thus, the absence of a long-term
527 increase in GPP and growth would not mean that enhanced [CO_2] was not beneficial for
528 model outputs (particularly in the case of C-source limitation) but that the net control
529 exerted by other factors such as climatically driven stress was more limiting than that of
530 [CO_2] availability: growth and photosynthesis would have been lower had we used
531 constant [CO_2] with the same model parameters. The absence of any modification in the

532 growth trends, even if there are changes in WUE, would express sink limitation mostly
533 related to hydraulic constraints (Peñuelas et al. 2011; Sala et al. 2012; Keenan et al.
534 2013). Often, the trees express a growth decline at those sites where there is an
535 enhancement in long-term water stress that dominates species performance (e.g. Bigler
536 et al. 2006; Piovesan et al. 2008; Gea-Izquierdo et al. 2014). In contrast, it has been
537 observed under certain conditions that trees have increased growth with warming since
538 the 1850s (Salzer et al. 2009; Gea-Izquierdo & Cañellas 2014). These studies suggest
539 the existence of a positive effect of warming rather than that of CO_2 fertilization upon
540 growth in forests where water stress is not the most limiting factor. Our study sites are
541 located within the Northern limit of the Mediterranean Region, meaning that the two
542 species studied occupy drier and warmer areas more to the South. The two species have
543 different functional characteristics, e.g. oaks are anisohydric whereas pines tend to be
544 isohydric. This confers them different capacities of adaptation to climate change, which
545 means that they should play different roles in future stand dynamics. Our results express
546 the existence of trade-offs in response to climate at different phenological periods. This
547 is important since synergistic environmental stresses acting at different periods can
548 trigger tree mortality (McDowell et al. 2013; Voltas et al. 2013). Model sensitivity
549 analysis could be performed to discuss the influence of specific factors such as climate
550 or [CO_2] causing instability in the climate-growth response (D'Arrigo et al. 2008;
551 Boucher et al. 2014). However [CO_2] enhancement and climate warming are mixed in
552 analysis performed using data from field studies, which can make the isolation of their
553 effect problematic. The model can be applied using abundant dendrochronological data
554 used to determine the site-dependent parameters. This would give much flexibility to
555 investigate growth trends and forest performance in response to global change at a
556 larger scale.

Conclusions

By developing an original process-based model with carbon allocation relationships explicitly expressed as functions of climate we accurately simulated gross primary productivity and allocation of carbon to secondary growth in evergreen Mediterranean forests. Different processes were modelled as functions of environmental variability, including [CO_2] and climate. The studied forests expressed trade-offs in carbon allocation to different plant compartments in response to stress in different seasons, namely with low temperatures and a short photoperiod in winter, and with moisture shortage in summer. We modelled a decreasing time trend in stomatal conductance, which would suggest a partly active increase of iWUE in the forests studied. Interannual variability in WUE followed closely that of iWUE. However, WUE exhibited a decreasing trend at the site where we simulated a decrease in LAI and GPP in response to a decrease in annual precipitation since the 1980s. Long-term GPP remained at similar levels in the last 50 years just in one stand whereas it declined in the forest suffering a reduction in precipitation. This suggests different acclimation processes at the canopy level and in the pattern of allocation in response to enhanced xericity and increasing [CO_2] levels, which could not counterbalance the negative effect of warming just in the site where there was a simultaneous decrease in precipitation. Tree growth was partly decoupled from stand productivity, highlighting that it can be risky to accept growth as a direct proxy to GPP. The model is flexible enough to assess both C-source and C-sink limitations and includes a dynamic estimation of stored C. These features would improve ecosystem models with a fixed C-source formulation. By calibrating a limited number of parameters related to carbon allocation the model has great potential to be used with abundant dendroecological data to characterise past instability in the

582 growth response in relation to environmental variability and simulate future forest
583 response under different climatic scenarios.
584
585 **Acknowledgements**
586 G.G.I was funded by the Labex OT-Med (n° ANR-11-LABEX-0061) from the
587 «Investissements d'Avenir» program of the French National Research Agency through
588 the A*MIDEX project (n° ANR-11-IDEX-0001-02). Federation de Recherche FR3098
589 ECCOREV, the labex IRDHEI and OHM-BMP also supported the study. We are
590 grateful to Roland Huc for sharing data from Fontblanche.
591
592 **References**
593 Allard, V., Ourcival, J. M., Rambal, S., Joffre, R. and Rocheteau, A.: Seasonal and
594 annual variation of carbon exchange in an evergreen Mediterranean forest in
595 southern France, Glob. Chang. Biol., 14(4), 714–725, 2008.
596 Baldocchi DD: Assessing the eddy covariance technique for evaluating carbon dioxide
597 exchange rates of ecosystems: Past, present and future. Glob. Chang. Biol., 9, 479–
598 492, 2003.
599 Baldocchi, D. D., Ma, S. Y., Rambal, S., Misson, L., Ourcival, J. M., Limousin, J. M.,
600 Pereira, J. and Papale, D.: On the differential advantages of evergreenness and
601 deciduousness in mediterranean oak woodlands: a flux perspective, Ecol. Appl.,
602 20(6), 1583–1597, 2010.
603 Beer, C., Ciais, P., Reichstein, M., Baldocchi, D., Law, B. E., Papale, D., Soussana, J.-
604 F., Ammann, C., Buchmann, N., Frank, D., Gianelle, D., Janssens, I. a., Knohl, a.,
605 Köstner, B., Moors, E., Roupsard, O., Verbeeck, H., Vesala, T., Williams, C. a. and

606 Wohlfahrt, G.: Temporal and among-site variability of inherent water use efficiency
607 at the ecosystem level, Global Biogeochem. Cycles, 23(2), 2009.
608 Bernacchi, C. J., Singsaas, E. L., Pimentel, C., Portis, A. R. and Long, S. P.: Improved
609 temperature response functions for models of Rubisco-limited photosynthesis, Plant
610 Cell Environ., 24(2), 253–259, 2001.
611 Bigler, C., Braker, O. U., Bugmann, H., Dobbertin, M. and Rigling, A.: Drought as an
612 inciting mortality factor in Scots pine stands of the Valais, Switzerland,
613 Ecosystems, 9(3), 330–343, 2006.
614 Boucher, É., Guiot, J., Hatté, C., Daux, V., Danis, P. -a. and Dussouillez, P.: An inverse
615 modeling approach for tree-ring-based climate reconstructions under changing
616 atmospheric CO_2 concentrations, Biogeosciences, 11(12), 3245–3258, 2014.
617 Breda, N., Huc, R., Granier, A. and Dreyer, E.: Temperate forest trees and stands under
618 severe drought: a review of ecophysiological responses, adaptation processes and
619 long-term consequences, Ann. For. Sci., 63(6), 625–644, 2006.
620 Breshears, D. D., Myers, O. B., Meyer, C. W., Barnes, F. J., Zou, C. B., Allen, C. D.,
621 McDowell, N. G. and Pockman, W. T.: Tree die-off in response to global change-
622 type drought: mortality insights from a decade of plant water potential
623 measurements, Front. Ecol. Environ., 7(4), 185–189, 2009.
624 Chen, G., Yang, Y. and Robinson, D.: Allocation of gross primary production in forest
625 ecosystems: allometric constraints and environmental responses. New Phytol.,
626 200(1176-1186), 2013.
627 D'Arrigo, R., Wilson, R., Liepert, B. and Cherubini, P.: On the "Divergence Problem"
628 in Northern Forests: A review of the tree-ring evidence and possible causes, Glob.
629 Planet. Change, 60(3-4), 289–305, 2008.

630 De Pury, D.G.G. and Farquhar, G.D.: Simple scaling of photosynthesis from leaves to
631 canopies without the errors of big-leaf models. Plant Cell Environ., 20(5), 537–557,
632 1997.
633 De Kauwe, M. G., Medlyn, B. E., Zaehle, S., Walker, A. P., Dietze, M. C., Hickler, T.,
634 Jain, A. K., Luo, Y. Q., Parton, W. J., Prentice, I. C., Smith, B., Thornton, P. E.,
635 Wang, S. S., Wang, Y. P., Warlind, D., Weng, E. S., Crous, K. Y., Ellsworth, D. S.,
636 Hanson, P. J., Seok Kim, H., Warren, J. M., Oren, R. and Norby, R. J.: Forest water
637 use and water use efficiency at elevated CO_2: a model-data intercomparison at two
638 contrasting temperate forest FACE sites, Glob. Chang. Biol., 19(6), 1759–1779,
639 2013.
640 Dickman, L. T., McDowell, N. G., Sevanto, S., Pangle, R. E. and Pockman, W. T.:
641 Carbohydrate dynamics and mortality in a piñon-juniper woodland under three
642 future precipitation scenarios., Plant. Cell Environ., 2014.
643 Evans, M. N., Reichert, B. K., Kaplan, A., Anchukaitis, K. J., Vaganov, E. A., Hughes,
644 M. K. and Cane, M. A.: A forward modeling approach to paleoclimatic
645 interpretation of tree-ring data, J. Geophys. Res., 111(G3), 2006.
646 Farquhar, G.D., von Caemmerer, S. and Berry, J.A.: A biochemical model of
647 photosynthetic CO_2 assimilation in leaves of C3 species, Planta, 149(1), 78–90,
648 1980.
649 Fatichi, S., Leuzinger, S. and Körner, C.: Moving beyond photosynthesis : from carbon
650 source to sink-driven vegetation modeling, New Phytol., 201, 1086–1095, 2013.
651 Flexas, J., Bota, J., Galmes, J., Medrano, H. and Ribas-Carbo, M.: Keeping a positive
652 carbon balance under adverse conditions: responses of photosynthesis and
653 respiration to water stress, Physiol. Plant., 127(3), 343–352, 2006.

Friedlingstein, P., Joel, G., Field, C. B. and Fung, I. Y.: Toward an allocation scheme for global terrestrial carbon models, Glob. Chang. Biol., 5(7), 755–770, 1999.

Fritts, H.C,: Tree Rings and Climate. Blackburn Press, 567 p, 1976

Gaucherel, C., Campillo, F., Misson, L., Guiot, J. and Boreux, J. J.: Parameterization of a process-based tree-growth model: Comparison of optimization, MCMC and Particle Filtering algorithms, Environ. Model. Softw., 23(10-11), 1280–1288, 2008.

Gea-Izquierdo, G., Mäkelä, A., Margolis, H., Bergeron, Y., Black, T. A., Dunn, A., Hadley, J., Kyaw Tha Paw U, Falk, M., Wharton, S., Monson, R., Hollinger, D. Y., Laurila, T., Aurela, M., McCaughey, H., Bourque, C., Vesala, T. and Berninger, F.: Modeling acclimation of photosynthesis to temperature in evergreen conifer forests. New Phytol., 188(1), 175–186, 2010.

Gea-izquierdo, G., Fernández-de-uña, L., Cañellas, I. Growth projections reveal local vulnerability of Mediterranean oaks with rising temperatures. For. Ecol. Manage., 305, 282–293, 2013.

Gea-Izquierdo, G. and Cañellas, I.: Long-term climate forces instability in long-term productivity of a Mediterranean oak along climatic gradients. Ecosystems, 17, 228–241, 2014.

Gea-Izquierdo, G., Viguera, B., Cabrera, M., Cañellas, I. Drought induced decline could portend widespread oak mortality at the xeric ecotone in managed Mediterranean pine-oak woodlands. Forest Ecol. Manag. 320, 70-82, 2014.

Granier, A., Breda, N., Longdoz, B., Gross, P. and Ngao, J.: Ten years of fluxes and stand growth in a young beech forest at Hesse, North-eastern France, Ann. For. Sci., 64 (7), 704, 2008.

677 Grassi, G. and Magnani, F.: Stomatal, mesophyll conductance and biochemical
678 limitations to photosynthesis as affected by drought and leaf ontogeny in ash and
679 oak trees, Plant, Cell Environ., 28(7), 834–849, 2005.
680 Guiot, J., Boucher, E. and Gea-Izquierdo, G.: Process models and model-data fusion in
681 dendroecology, Front. Ecol. Evol., 2(August), 1–12, 2014.
682 Hoff, C. and Rambal, S.: An examination of the interaction between climate, soil and
683 leaf area index in a Quercus ilex ecosystem, Ann. For. Sci., 60(2), 153–161, 2003.
684 IPCC. Climate Change: The Physical Science Basis. Summary for policymakers.
685 Stocker, T.F. et al. (Eds.) IPCC, Geneva, Switzerland. pp 33. 2013.
686 Keenan, T., Maria Serra, J., Lloret, F., Ninyerola, M. and Sabate, S.: Predicting the
687 future of forests in the Mediterranean under climate change, with niche- and
688 process-based models: CO_2 matters!, Glob. Chang. Biol., 17(1), 565–579, 2011.
689 Keenan, T. F., Hollinger, D. Y., Bohrer, G., Dragoni, D., Munger, J. W., Schmid, H. P.
690 and Richardson, A. D.: Increase in forest water-use efficiency as atmospheric
691 carbon dioxide concentrations rise., Nature, 499(7458), 324–7, 2013.
692 Koenig, W. D. and Knops, M. H.: Patterns of annual seed production by Northern
693 Hemisphere trees: a global perspective., Am. Nat., 155(1), 59–69, 2000.
694 Körner, C., Basel, M.L. Growth Controls Photosynthesis – Mostly. Nova Acta
695 Leopoldina, 283, 273–283, 2013.
696 Leonardi, S., Gentilesca, T., Guerrieri, R., Ripullone, F., Magnani, F., Mencuccini, M.,
697 Noije, T. V and Borghetti, M.: Assessing the effects of nitrogen deposition and
698 climate on carbon isotope discrimination and intrinsic water-use efficiency of
699 angiosperm and conifer trees under rising CO_2 conditions, Glob. Chang. Biol.,
700 18(9), 2925–2944, 2012.

Le Roux, X., Lacointe, A., Escobar-Gutierrez, A. and Le Dizes, S.: Carbon-based models of individual tree growth: A critical appraisal, Ann. For. Sci., 58(5), 469–506, 2001.

Leuning, R.: A critical appraisal of a combined stomatal-photosynthesis model for C3 plants. Plant Cell Environ. 18, 339-355, 1995

Lévesque, M., Siegwolf, R., Saurer, M., Eilmann, B. and Rigling, A.: Increased water-use efficiency does not lead to enhanced tree growth under xeric and mesic conditions., New Phytol., 203(1), 94–109, 2014.

Li, G., Harrison, S. P., Prentice, I. C. and Falster, D.: Simulation of tree ring-widths with a model for primary production, carbon allocation and growth, Biogeosciences Discuss., 11(7), 10451–10485, 2014.

Limousin, J. M., Rambal, S., Ourcival, J. M., Rocheteau, A., Joffre, R. and Rodriguez-Cortina, R.: Long-term transpiration change with rainfall decline in a Mediterranean *Quercus ilex* forest, Glob. Chang. Biol., 15(9), 2163–2175, 2009.

Limousin, J. M., Longepierre, D., Huc, R. and Rambal, S.: Change in hydraulic traits of Mediterranean *Quercus ilex* subjected to long-term throughfall exclusion, Tree Physiol., 30(8), 1026–1036, 2010.

Limousin, J.-M., Rambal, S., Ourcival, J.-M., Rodriguez-Calcerrada, J., Perez-Ramos, I. M., Rodriguez-Cortina, R., Misson, L. and Joffre, R.: Morphological and phenological shoot plasticity in a Mediterranean evergreen oak facing long-term increased drought, Oecologia, 169(2), 565–577, 2012.

Maseyk, K. S., Lin, T., Rotenberg, E., Grünzweig, J. M., Schwartz, A. and Yakir, D.: Physiology-phenology interactions in a productive semi-arid pine forest., New Phytol., 178(3), 603–16, 2008.

McDowell, N.G., Fisher, R.A., Xu, C., Domec, J., Hölttа, T., Mackay, D.S., Sperry, J. S., Boutz, A., Dickman, L., Gehres, N., Limousin, J.M., Macalady, A., Pangle, R. E., Rasse, D.P., Ryan, M.G., Sevanto, S., Waring, R.H., Williams, A.P., Yepez, E. A. and Pockman, W.T.: Evaluating theories of drought-induced vegetation mortality using a multimodel – experiment framework, New Phytol., 200, 304–321, 2013.

McMurtrie, R. E. and Dewar, R. C.: New insights into carbon allocation by trees from the hypothesis that annual wood production is maximized, New Phytol., 199(4), 981–990, 2013.

Millard, P., Sommerkorn, M., Grelet, G.A. Environmental change and carbon limitation in trees: A biochemical, ecophysiological and ecosystem appraisal. New Phytologist, 175, 11–28, 2007.

Misson, L.: MAIDEN: a model for analyzing ecosystem processes in dendroecology. Can. J. For. Res., 34, 874–887, 2004.

Misson, L., Rathgeber, C. and Guiot, J.: Dendroecological analysis of climatic effects on Quercus petraea and Pinus halepensis radial growth using the process-based MAIDEN model, Can. J. For. Res., 34(4), 888–898, 2004.

Misson, L., Tang, J., Xu, M., Mckay, M. and Goldstein, A.: Influences of recovery from clear-cut , climate variability , and thinning on the carbon balance of a young ponderosa pine plantation, Agric. Fore, 130, 207–222, 2005.

Misson, L., Degueldre, D., Collin, C., Rodriguez, R., Rocheteau, A., Ourcival, J.-M. and Rambal, S.: Phenological responses to extreme droughts in a Mediterranean forest, Glob. Chang. Biol., 17(2), 1036–1048, 2011.

Montserrat-Marti, G., Camarero, J. J., Palacio, S., Perez-Rontome, C., Milla, R., Albuixech, J. and Maestro, M.: Summer-drought constrains the phenology and growth of two coexisting Mediterranean oaks with contrasting leaf habit:

implications for their persistence and reproduction, Trees-Structure Funct., 23(4), 787–799, 2009.

Niinemets, U.: Photosynthesis and resource distribution through plant canopies., Plant. Cell Environ., 30(9), 1052–71, 2007.

Niinemets, U. and Valladares, F.: Photosynthetic acclimation to simultaneous and interacting environmental stresses along natural light gradients: optimality and constraints., Plant Biol. (Stuttg)., 6(3), 254–68, 2004.

Niinemets, Ü., Tenhunen, J. D., Canta, N. R., Chaves, M. M., Faria, T., Pereira, J. S. and Reynolds, J. F.: Interactive effects of nitrogen and phosphorus on the acclimation potential of foliage photosynthetic properties of cork oak, *Q. suber*, to elevated atmospheric CO_2 concentrations, Glob. Chang. Biol., 5, 455–470, 1999.

Nobel, P.S.: Physicochemical and environmental plant physiology. 4th edn. Academic Press, Elsevier, Oxford UK, 2009.

Peng, C. H., Guiot, J., Wu, H. B., Jiang, H. and Luo, Y. Q.: Integrating models with data in ecology and palaeoecology: advances towards a model-data fusion approach, Ecol. Lett., 14(5), 522–536, 2011.

Peñuelas, J., Hunt, J. M., Ogaya, R. and Jump, A. S.: Twentieth century changes of tree-ring delta C-13 at the southern range-edge of Fagus sylvatica: increasing water-use efficiency does not avoid the growth decline induced by warming at low altitudes, Glob. Chang. Biol., 14(5), 1076–1088, 2008.

Peñuelas, J., Canadell, J. G. and Ogaya, R.: Increased water-use efficiency during the 20th century did not translate into enhanced tree growth, Glob. Ecol. Biogeogr., 20(4), 597–608, 2011.

Pereira, J. S., Mateus, J. A., Aires, L. M., Pita, G., Pio, C., David, J. S., Andrade, V., Banza, J., David, T. S., Paco, T. A. and Rodrigues, A.: Net ecosystem carbon

exchange in three contrasting Mediterranean ecosystems - the effect of drought, Biogeosciences, 4(5), 791–802, 2007.

Pérez-Ramos, I. M., Ourcival, J. M., Limousin, J. M. and Rambal, S.: Mast seeding under increasing drought: results from a long-term data set and from a rainfall exclusion experiment, Ecology, 91(10), 3057–3068, 2010.

Piovesan, G., Biondi, F., Di Filippo, A., Alessandrini, A. and Maugeri, M.: Drought-driven growth reduction in old beech (*Fagus sylvatica* L.) forests of the central Apennines, Italy, Glob. Chang. Biol., 14(6), 1265–1281, 2008.

Rambal, S., Joffre, R., Ourcival, J. M., Cavender-Bares, J. and Rocheteau, a.: The growth respiration component in eddy CO2 flux from a *Quercus ilex* mediterranean forest, Glob. Chang. Biol., 10(9), 1460–1469, 2004.

Reichstein, M., Tenhunen, J. D., Roupsard, O., Ourcival, J. M., Rambal, S., Miglietta, F., Peressotti, A., Pecchiari, M., Tirone, G. and Valentini, R.: Severe drought effects on ecosystem CO_2 and H_2O fluxes at three Mediterranean evergreen sites: revision of current hypotheses?, Glob. Chang. Biol., 6(10), 999–1017, 2002.

Reichstein, M., Tenhunen, J., Roupsard, O., Ourcival, J. M., Rambal, S., Miglietta, F., Peressotti, A., Pecchiari, M., Tirone, G. and Valentini, R.: Inverse modeling of seasonal drought effects on canopy CO2/H2O exchange in three Mediterranean ecosystems, J. Geophys. Res., 108(23), 2003.

Reichstein, M., Falge, E., Baldocchi, D., Papale, D., Aubinet, M., Berbigier, P., Bernhofer, C., Buchmann, N., Gilmanov, T., Granier, A., GruÌˆnwald, T., HavraÌ nkovaÌ , K., Ilvesniemi, H., Janous, D., Knohl, A., Laurila, T., Lohila, A., Loustau, D., Matteucci, G., Meyers, T., Miglietta, F., Ourcival, J. M., Pumpanen, J., Rambal, S., Rotenberg, E., Sanz, M., Tenhunen, J., Seufert, G., Vaccari, F., Vesala, T., Yakir, D. and Valentini, R.: On the separation of net

ecosystem exchange into assimilation and ecosystem respiration: Review and improved algorithm, Glob. Chang. Biol., 11(9), 1424–1439, 2005.

Sala, A. and Tenhunen, J. D.: Simulations of canopy net photosynthesis and transpiration in *Quercus ilex* L . under the influence of seasonal drought, Agric. For. Meteorol., 78 203–222, 1996.

Sala, A., Woodruff, D. R. and Meinzer, F. C.: Carbon dynamics in trees: feast or famine?, Tree Physiol., 32(6), 764–75, 2012.

Salzer, M. G., Hughes, M. K., Bunn, A. G. and Kipfmueller, K. F.: Recent unprecedented tree-ring growth in bristlecone pine at the highest elevations and possible causes., PNAS, 106(48), 20348–20353, 2009.

Saurer, M., Spahni, R., Frank, D.C., Joos, F., Leuenberger, M., Loader, N.J., McCarroll, D., Gagen, M., Poulter, B., Siegwolf, R. T. W., Andreu-Hayles, L., Boettger, T., Dorado, I., Fairchild, I. J., Friedrich, M., Gutierrez, E., Haupt, M., Hilasvuori, E., Heinrich, I., Helle, G., Grudd, H., Jalkanen, R., Levanič, T., Linderholm, H. W., Robertson, I., Sonninen, E., Treydte, K., Waterhouse, J. S., Woodley, E. J., Wynn, P. M. and Young, G. H. F.: Spatial variability and temporal trends in water-use efficiency of European forests., Glob. Chang. Biol., 3700–3712, 2014.

Schaefer, K., Schwalm, C.R., Williams, C., Arain, M.A., Barr, A., Chen, J.M., Davis, K. J., Dimitrov, D., Hilton, T.W., Hollinger, D.Y., Humphreys, E., Poulter, B., Raczka, B.M., Richardson, A.D., Sahoo, A., Thornton, P., Vargas, R., Verbeeck, H., Anderson, R., Baker, I., Black, T.A., Bolstad, P., Chen, J., Curtis, P.S., Desai, A. R., Dietze, M., Dragoni, D., Gough, C., Grant, R. F., Gu, L., Jain, A., Kucharik, C., Law, B., Liu, S., Lokipitiya, E., Margolis, H.A., Matamala, R., McCaughey, J. H., Monson, R., Munger, J.W., Oechel, W., Peng, C., Price, D. T., Ricciuto, D., Riley, W. J., Roulet, N., Tian, H., Tonitto, C., Torn, M., Weng, E. and Zhou, X.: A

825 model-data comparison of gross primary productivity: Results from the North
826 American Carbon Program site synthesis, J. Geophys. Res., 117(G3), G03010,
827 2012.
828 Simioni, G., Durand-Gillmann, M. and Huc, R.: Asymmetric competition increases leaf
829 inclination effect on light absorption in mixed canopies, Ann. For. Sci., 70(2), 123–
830 131, 2013.
831 Sun, Y., Gu, L., Dickinson, R. E., Norby, R. J., Pallardy, S. G. and Hoffman, F. M.:
832 Impact of mesophyll diffusion on estimated global land CO 2 fertilization, Proc.
833 Natl. Acad. Sci. U. S. A., 111(44), 15774–15779, 2014.
834 Tolwinski-Ward, S. E., Evans, M. N., Hughes, M. K. and Anchukaitis, K. J.: An
835 efficient forward model of the climate controls on interannual variation in tree-ring
836 width, Clim. Dyn., 36(11-12), 2419–2439, 2011.
837 Touchan, R., Shishov, V. V, Meko, D. M., Nouiri, I. and Grachev, A.: Process based
838 model sheds light on climate sensitivity of Mediterranean tree-ring width,
839 Biogeosciences, 9(3), 965–972, 2012.
840 Vaganov, E.A., Hughes, M.K., Shashkin, A.V. Growth Dynamics of Conifer Tree
841 Rings: Images of Past and Future Environments. Springer, New York. 2006.
842 Vaz, M., Pereira, J. S., Gazarini, L. C., David, T. S., David, J. S., Rodrigues, A.,
843 Maroco, J. and Chaves, M. M.: Drought-induced photosynthetic inhibition and
844 autumn recovery in two Mediterranean oak species (*Quercus ilex* and *Quercus*
845 *suber*), Tree Physiol., 30(8), 946–956, 2010.
846 Voltas, J., Camarero, J. J., Carulla, D., Aguilera, M., Ortiz, A. and Ferrio, J. P.: A
847 retrospective, dual-isotope approach reveals individual predispositions to winter-
848 drought induced tree dieback in the southernmost distribution limit of Scots pine.,
849 Plant. Cell Environ., 36(8), 1435–48, 2013.

850 **Table 1.** Characteristics of mean annual gross primary productivity, climatic (annual
851 means) and growth data. Standard deviations are shown between parentheses.
852 Precipitation=mean annual precipitation; Tmax=annual mean of mean daily maximum
853 temperature; Tmin= annual mean of mean daily minimum temperature.
854 Length=chronology year replicated with more than 5 radii; RW=mean annual ring-
855 width; Rbs = mean correlation between series; AR = mean autocorrelation of raw series;
856 MS = mean sensitivity; EPS = mean expressed population signal Rbs, AR, MS and EPS
857 are classical statistics to characterise growth chronologies, and follow Fritts (1976).
858

		Fontblanche		Puechabon
Flux Data	Period	2008-2012		2001-2013
	GPP annual ($g\ C\ m^{-2}\ year^{-1}$)	1431.4 (305.4)		1207.3 (206.7)
Climate	Period	1964-2012		1954-2013
	Precipitation (mm)	642.7 (169.7)		1002.6 (328.2)
	Tmax (ºC)	20.6 (0.9)		17.8 (1.26)
	Tmin (ºC)	8.8 (0.5)		8.1 (0.8)
Growth Data	Species	*P. halepensis*	*Q. ilex*	*Q.ilex*
	# Trees/Radii	25/47	15/30	17/32
	Length	1910-2013	1941-2013	1941-2005
	RW (mm)	2.19 (1.1)	1.25 (0.7)	1.13 (0.7)
	MS	0.308	0.372	0.443
	AR	0.684	0.591	0.436
	Rbs	0.541	0.281	0.457
	EPS	0.963	0.884	0.949

859

860 **Table 2**. Model parameters. Those parameter differing between sites were optimized
861 either with GPP data (photosynthesis and allocation module) or with growth-based
862 biomass increment chronologies (allocation module). The rest were common parameters
863 for both sites and selected while developing the model in the first step for Fontblanche
864 using GPP data (represented in 'Cal' with a '-'). Meaning of parameters, equation
865 number (E#) and phenophase [P#] are as in the text in Material and Methods.
866 Fontb=Fontblanche; Puech=Puechabon; Cal=local parameters to be calibrated with GPP
867 or stem biomass increment data (SBI).

868

Process	Process/Equation #	Parameter		Fontb	Puech	Units	Cal
Photosynthesis	Leaf photosynthesis [E2]	J_{coef}	QUIL	1.59		µmol C m^{-2} s^{-1}	-
			PIHA	1.44	-		
	Leaf photosynthesis [E3]	V_{max}	QUIL	32.3		µmol C m^{-2} s^{-1}	-
			PIHA	46.0	-		
		V_b	QUIL	-0.106		ºC^{-1}	-
			PIHA	-0.180	-		
		V_{ip}	QUIL	13.7		ºC	-
			PIHA	20.0	-		
	Stress V_{cmax} [E4]	p_{str}		-0.05		mm^{-1}	-
	Stomatal conductance [E5]	g_1	QUIL	7.5		-	-
			PIHA	6.1	-		
		VPD_0		30000		Pa	-
	Water stress [E6]	$Soil_b$		-0.054		mm^{-1}	-
		$Soil_{ip}$		22.2	81.8	mm	GPP
Allocation	Respiration [E7]	p_{respi}		-0.225		ºC^{-1}	-
	Stress LAI [E8]	p_{LAI}		65.5		mm	-
	[P2]	GDD_1		203.3		ºC	-
	Stored carbon buds [P3]	C_{bud}		7		g C day^{-1}	-
	[P5]	Photoperiod		9.5		hours	-
	Allocation canopy [P3], [E9]	st_{4moist}		-0.089	-0.173	mm^{-1}	GPP
		st_{4temp}		53.3	75	ºC	GPP
		st_{4sd}		26.9	26.1	ºC	GPP
	Allocation stem [P3], [E10]	st_{3moist}		-0.045	-0.117	mm^{-1}	SBI
		st_{3temp}		32.9	6.3	ºC	SBI
		st_{3sd}		38.0	3.0	ºC	SBI
	Allocation stor/stem [P4], [E11]	st_{4moist}		200.8	119.3	mm	SBI
		st_{4temp}		0.060	-0.097	ºC^{-1}	SBI

869

Figure 1. Outline of the different phenological phases (P1 to P5) and carbon allocation in the model within a given year. A_n=net daily carbon assimilation; NSC=storage (non-structural carbohydrates); GDD=growing degree days, GDD_l=parameter determining shift from P2 to P3 (see text); C=carbon allocated either to the stem, canopy or roots; d=day of year. Solid arrows correspond to allocation within the plant whereas dashed arrows to correspond to litterfall (canopy or roots). f_3 and f_4 are nonlinear functions of soil water content and temperature determining carbon allocation to different compartments (see text for more details).

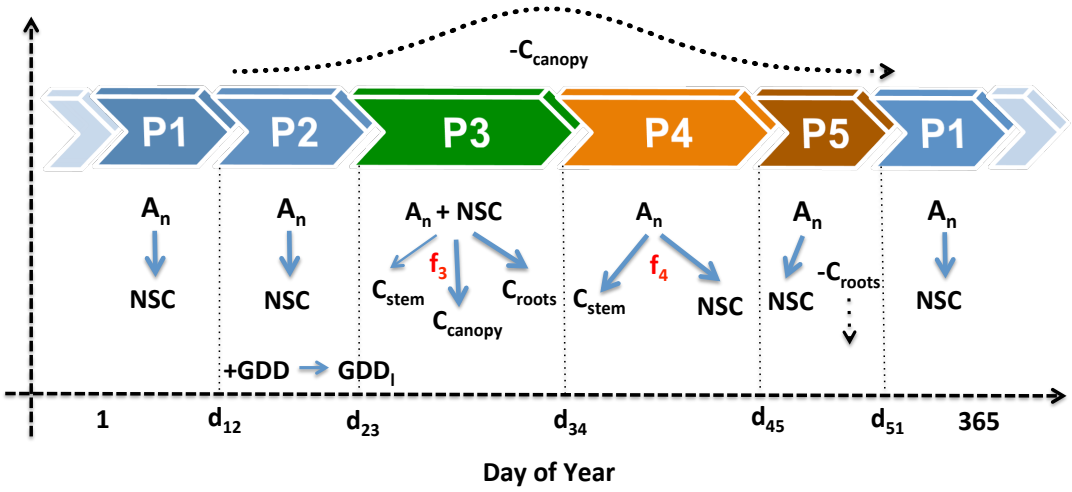

879 **Figure 2**. Growth (basal area increment, BAI, $cm^2 \cdot year^{-1}$) and biomass allocated to the
880 tree stem ($g\ C \cdot m^{-2} \cdot year^{-1}$) of *Q. ilex* and *P. halepensis* at Fontblanche (growth shown in
881 (a), biomass in (b)) and *Q. ilex* at Puechabon (growth and stem biomass shown in (c)).
882 A vertical dashed line marks the release event in Fontblanche produced by the enhanced
883 winter mortality in 1985 in (a). Dark lines for BAI correspond to yearly means while
884 grey polygons show confidence intervals (at 95%) on the standard errors of the mean.
885

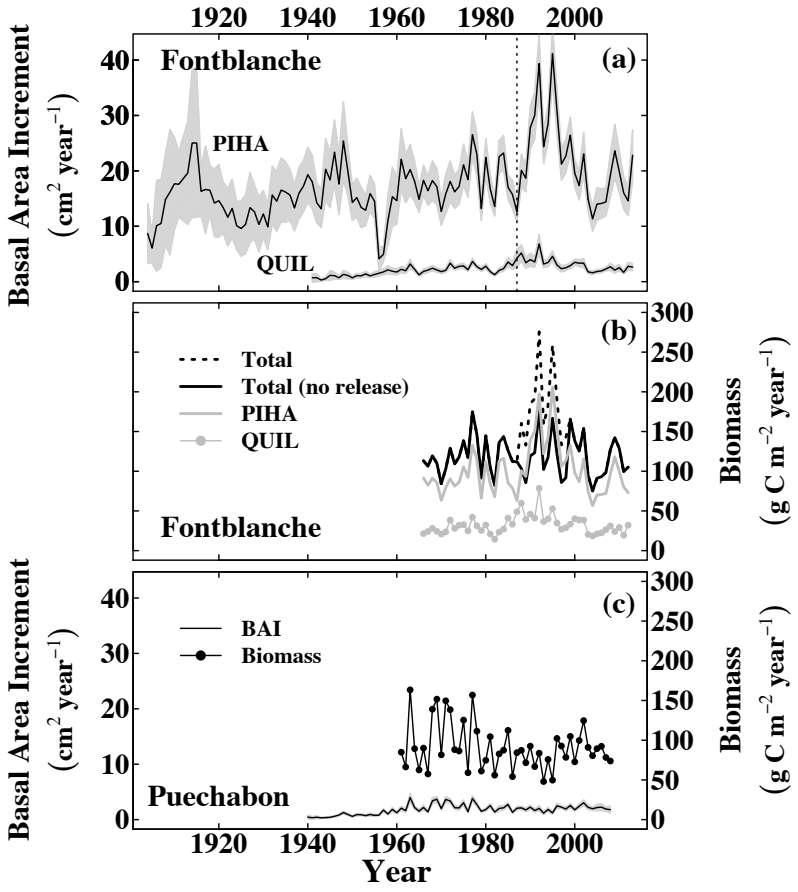

Figure 3. Daily gross primary productivity (GPP) at Puechabon (2001-2013, black dots, blue line) and Fontblanche (2008-2012, orange dots, red line). DOY=day of year. Thick lines correspond to smoothers fitted to the mean to highlight seasonal trends at the two sites.

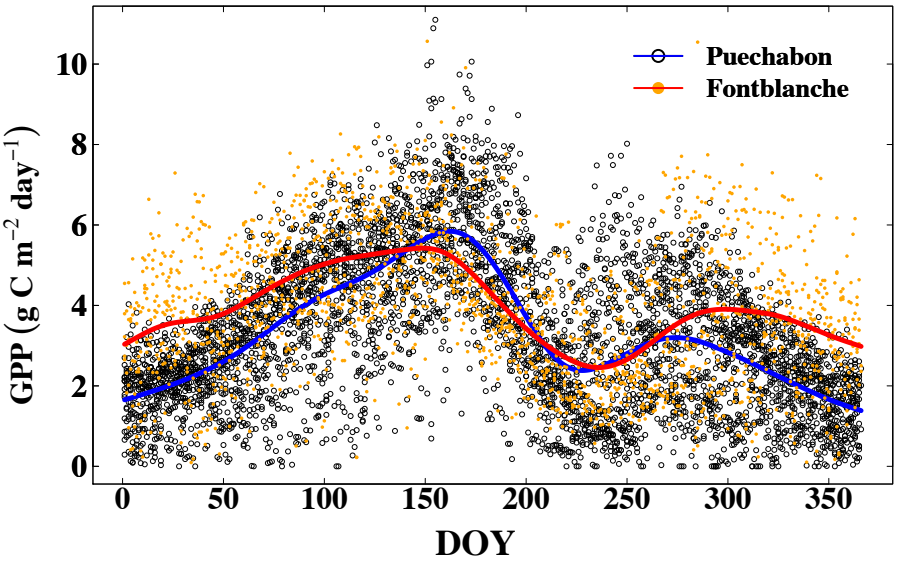

Figure 4. Model fit to stem biomass increment (a) and GPP (b) in Fontblanche; and stem biomass increment (c) and GPP (d) in Puechabon. R^2=coefficient of determination; ρ=linear correlation between estimated and observed data, ρ_{low15}=linear correlation between estimated and observed data smoothed with a 15 year low-pass filter (blue and red lines in (b) and (c)). Polygons behind the estimated values in (a) and (c) correspond to confidence intervals of the mean: solid grey polygons for estimated values and dashed polygons for observed stem biomass increment values.

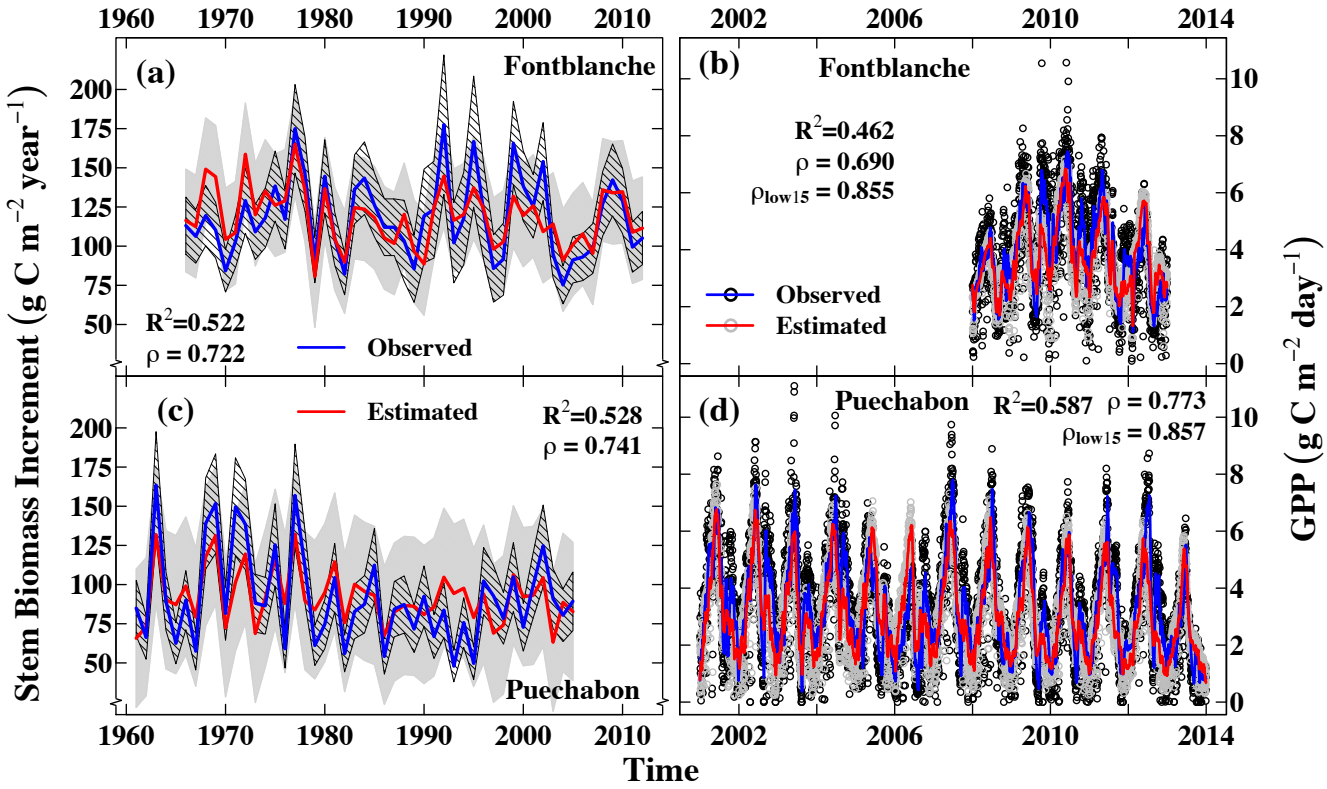

Figure 5. Modelled carbon allocation trajectory to the stem when leaf flush has finished in phenological period [P4]. We show the unitless modifier 1-h_4(i) (i.e. h_4(i) is the portion of allocated carbon to storage) from $C_{stem}(i) = A_N(i) \cdot [(1-h_4(i))]$ as from [E11]. The modifier [0,1] is a function of soil water content (SWC) and maximum temperature (Tmax) and multiplies available daily carbon to distribute daily carbon allocated between secondary growth and storage.

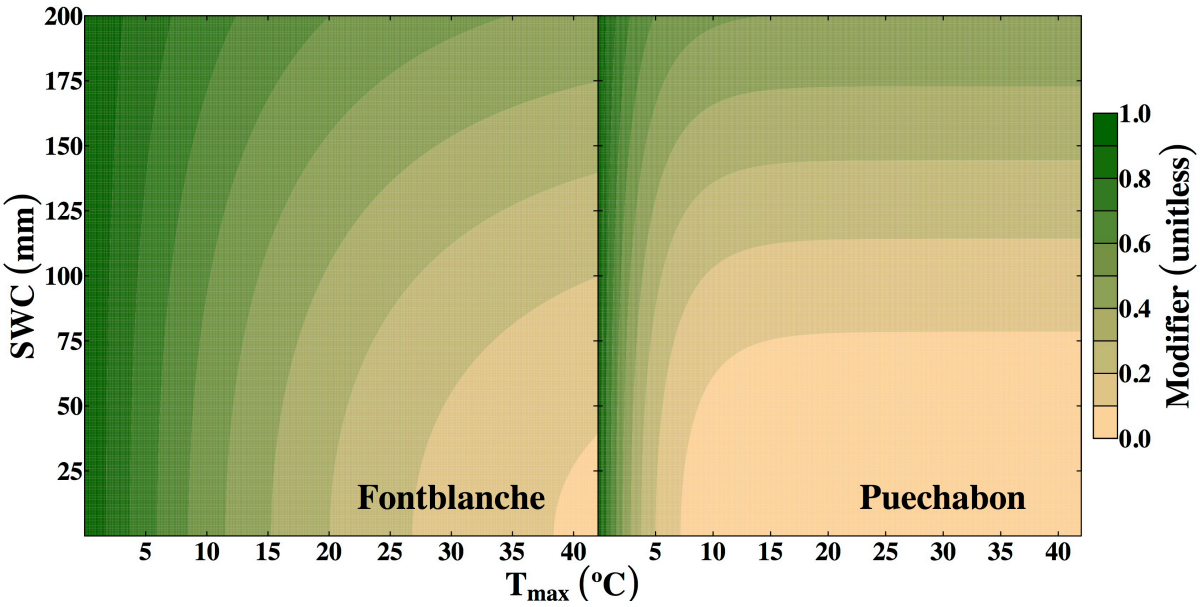

Figure 6. Modelled total annual stand gross primary productivity (GPP) and mean stomatal conductance of sunny leaves (gs) for Fontblanche (a) and Puechabon (b) for the period where meteorological data were available. To show the influence of the precipitation decline observed in Puechabon on GPP we run a sensitivity simulation where precipitation was set fixed for 1980-2012 as in 1960-1979 (Figure A1) and all other input variables (T_{min}, T_{max}, $[CO_2]$) were actual values. GPP values from this simulation are depicted as dashed grey lines in (b).

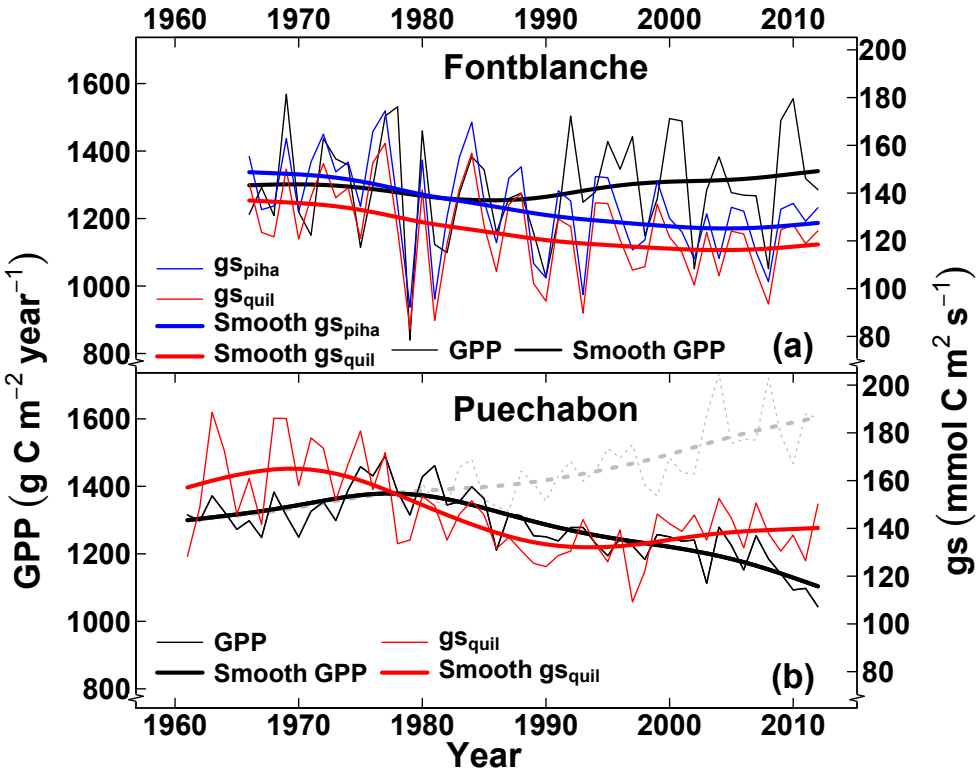

Figure 7. Ecosystem WUE (integral annual) and iWUE for sun leaves (mean daily, for PIHA and QUIL separated in Fontblanche) for (a) Fontblanche and (b) Puechabon for the period where we had available meteorological data.

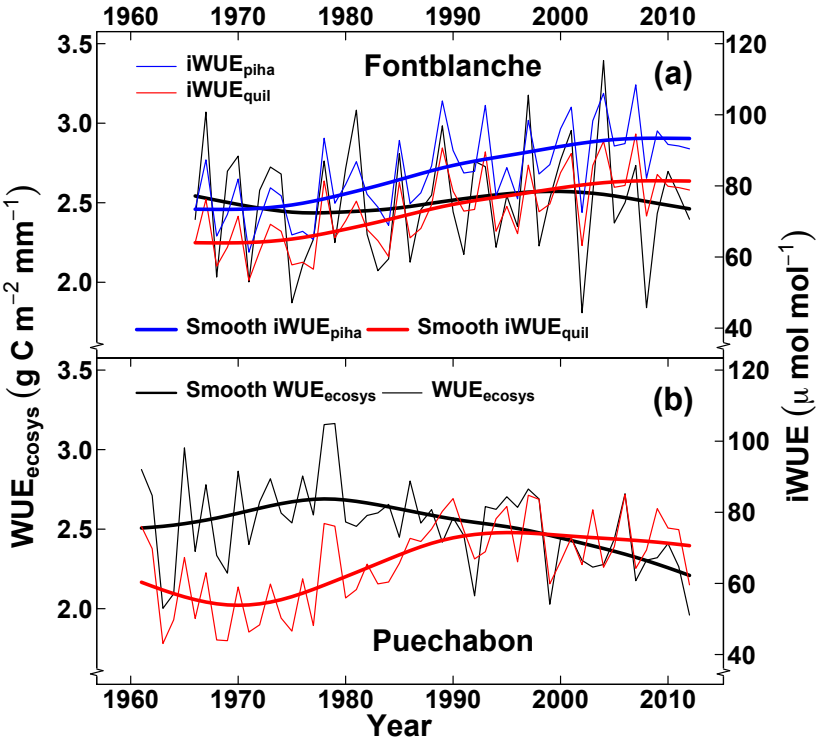

Figure A1. Mean climatic time series in the last 50 years. (a) annual precipitation; (b) and (c) annual maximum (Tmax) and minimum (Tmin) temperatures for Fontblanche (b) and Puechabon (c).

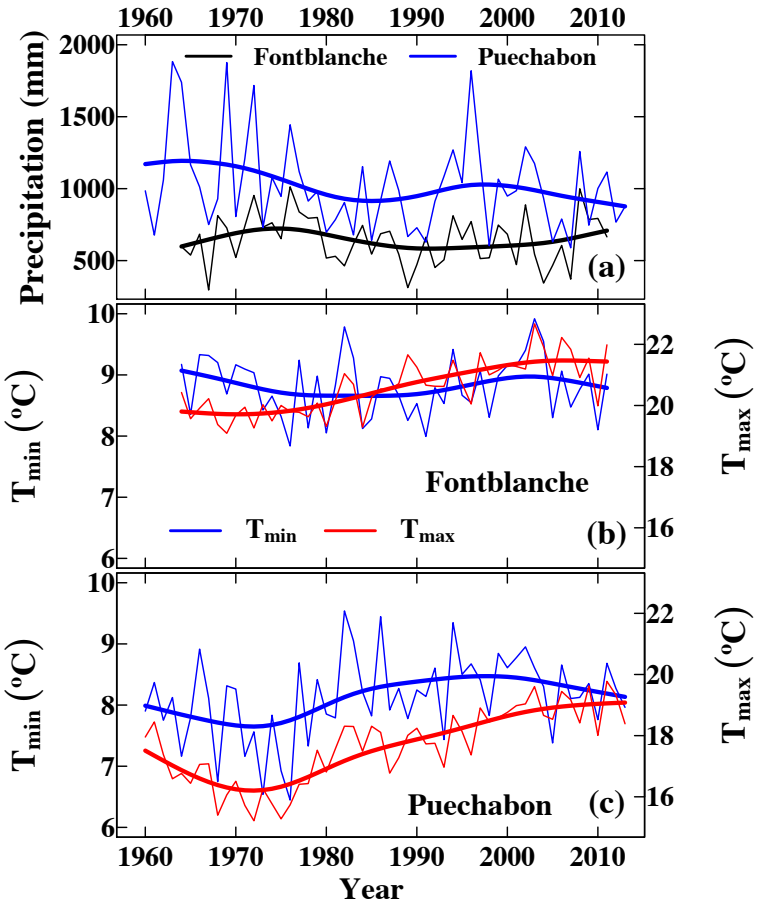

Figure A2. Diameter (dbh, cm) and age (years) distribution of trees included in the chonologies. Frequencies are calculated separately by species and site.

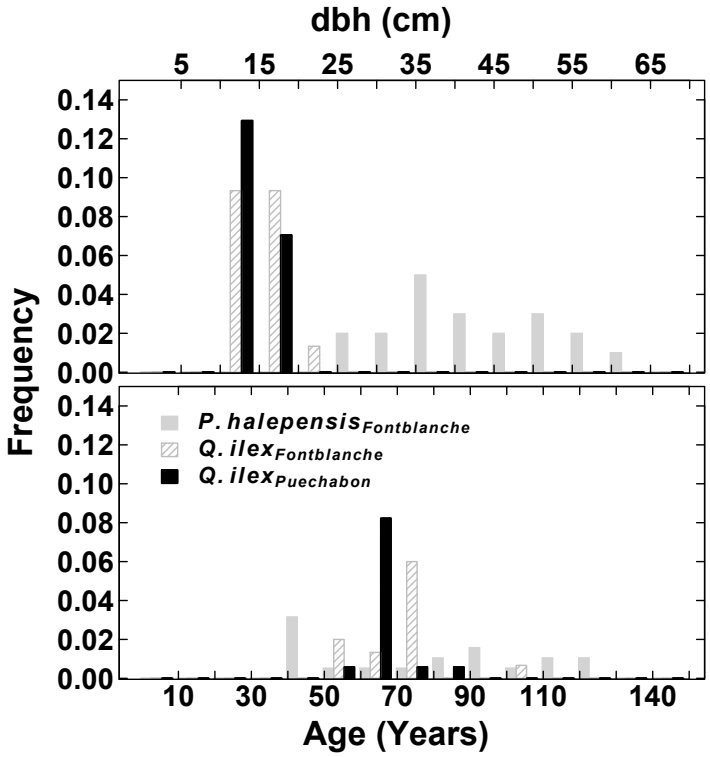

Figure A3. Simulated maximum annual leaf area index LAI ($m^2 \cdot m^{-2}$) and total annual stand transpiration E (mm/year) in Fontblanche (a) and Puechabon (b).

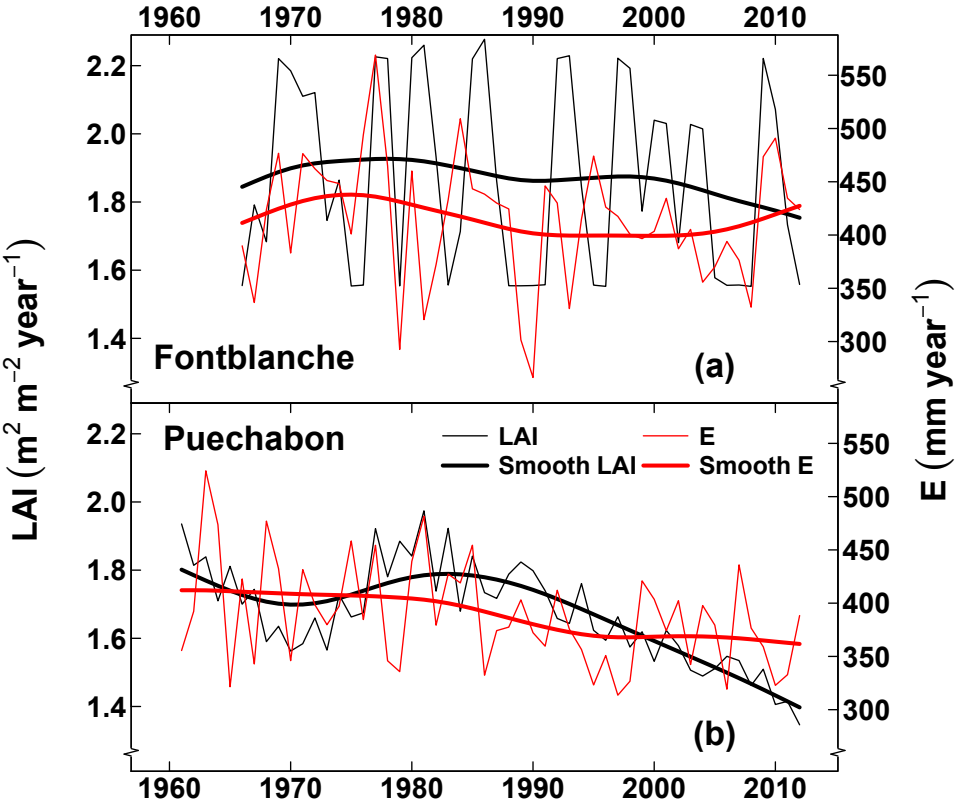

Figure A4. Simulated mean annual stomatal conductance (g_s) as a function of mean $[CO_2]$ (a) and mean maximum temperature (b).

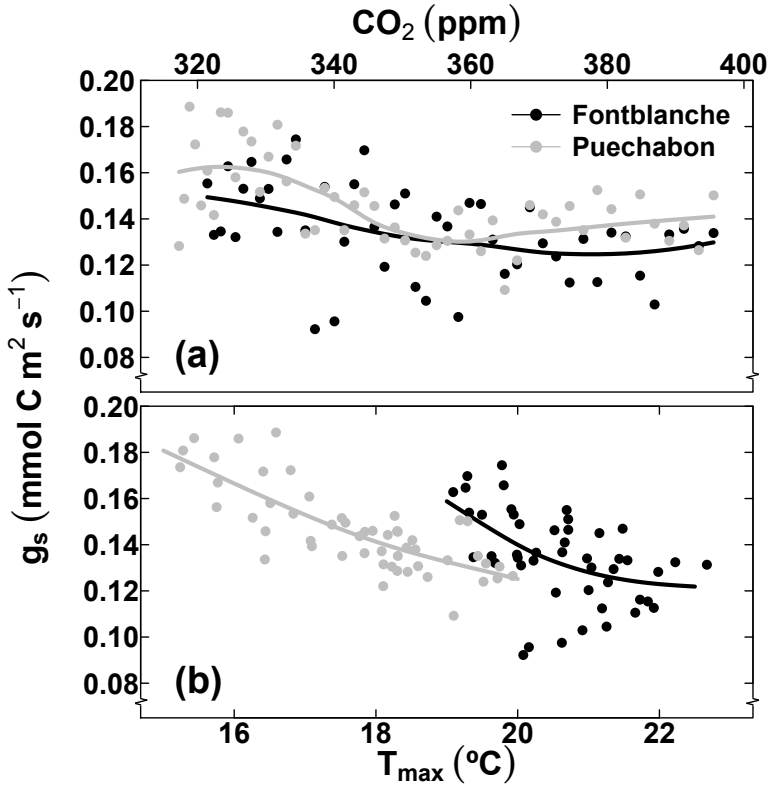

Figure A5. Simulated non-structural carbohydrate content (NSC) in the storage pool at both sites. The period 1995-2012 is shown to highlight within year variability.